

# Simultaneous transmission of 20x2 WDM/SCM-QKD and 4 bidirectional classical channels over a PON

J. Mora, W. Amaya, A. Ruiz-Alba, A. Martínez, D. Calvo, V. García Muñoz,  
and J. Capmany\*

*Institute of Telecommunications and Multimedia Applications (iTEAM), Universitat Politècnica de València, Camino de Vera S/N, 46021 Valencia- Spain*

*\*jcapmany@iteam.upv.es*

**Abstract:** We report the transmission of 40 quantum-key channels using WDM/SCM-QKD technology and 4 bidirectional classical channels over a PON. To our knowledge the highest number of quantum key channels simultaneously transmitted that has ever been reported. The quantum signal coexists with classical reference channel which is employed to process the qbits, but it has enough low power to avoid Raman crosstalk and achieving a high number of WDM-QKD channels. The experimental results allow us to determine the minimum rejection ratio required by the filtering devices employed to select each quantum channel and maximize the quantum key rate. These results open the path towards high-count QKD channel transmission over optical fiber infrastructures.

©2012 Optical Society of America

OCIS codes: (270.5568) Quantum cryptography; (060.4230) Multiplexing.

---

## References and links

1. N. Gisin, G. Ribordy, W. Tittel, and H. Zbinden, "Quantum cryptography," *Rev. Mod. Phys.* **74**(1), 145–195 (2002).
2. V. Scarani, H. Bechmann-Pasquinucci, N. J. Cerf, M. Dušek, N. Lütkenhaus, and M. Peev, "The security of practical quantum key distribution," *Rev. Mod. Phys.* **81**(3), 1301–1350 (2009).
3. J. Capmany and D. Novak, "Microwave photonics combines two worlds," *Nat. Photonics* **1**(6), 319–330 (2007).
4. J. Chen, G. Wu, L. Xu, X. Gu, E. Wu, and H. Zeng, "Stable quantum key distribution with active polarization control based on time-division multiplexing," *New J. Phys.* **11**(6), 065004 (2009).
5. K. Yoshino, M. Fujiwara, A. Tanaka, S. Takahashi, Y. Nambu, A. Tomita, S. Miki, T. Yamashita, Z. Wang, M. Sasaki, and A. Tajima, "A high-speed wavelength-division multiplexing quantum key distribution system," *Opt. Lett.* **37**(2), 223–225 (2012).
6. J. Mora, A. Ruiz-Alba, W. Amaya, A. Martínez, V. García-Muñoz, D. Calvo, and J. Capmany, "Experimental demonstration of subcarrier multiplexed quantum key distribution system," *Opt. Lett.* **37**(11), 2031–2033 (2012).
7. P. Townsend, "Simultaneous quantum cryptographic key distribution and conventional data transmission over installed fibre using wavelength-division multiplexing," *Electron. Lett.* **33**(3), 188–190 (1997).
8. A. Tanaka, M. Fujiwara, K. Yoshino, S. Takahashi, Y. Nambu, A. Tomita, S. Miki, T. Yamashita, Z. Wang, M. Sasaki, and A. Tajima, "A scalable full quantum key distribution system based on colourless interferometric technique and hardware key distillation," in *Proc. 37th European Conference on Optical Communication*, paper Mo.1.B.3, 1–3 (2011).
9. I. Choi, R. J. Young, and P. D. Townsend, "Quantum key distribution on a 10Gb/s WDM-PON," *Opt. Express* **18**(9), 9600–9612 (2010).
10. B. Ortega, J. Mora, G. Puerto, and J. Capmany, "Symmetric reconfigurable capacity assignment in a bidirectional DWDM access network," *Opt. Express* **15**(25), 16781–16786 (2007).
11. J. Mora, A. Ruiz-Alba, W. Amaya, V. García-Muñoz, A. Martínez, and J. Capmany, "Microwave photonic filtering scheme for BB84 subcarrier multiplexed quantum key distribution," in *IEEE Topical Meeting on Microwave Photonics*, pp. 286–289 (2007).
12. O. Guerreau, F. J. Malassenet, S. W. McLaughlin, and J. M. Merolla, "Quantum key distribution without a single-photon source using a strong reference," *IEEE Photon. Technol. Lett.* **17**(8), 1755–1757 (2005).
13. J. Capmany and C. R. Fernandez-Pousa, "Impact of third-order intermodulation on the performance of subcarrier multiplexed quantum key distribution," *J. Lightwave Technol.* **29**(20), 3061–3069 (2011).

## 1. Introduction

Quantum Key Distribution (QKD) techniques, which rely on exploiting the laws of quantum mechanics, can offer unconditional security without imposing any computational assumptions [1, 2] and at the same time are prone for practical implementation using standard photonic components. The functionality of QKD systems has been widely demonstrated and the last researches have been oriented to increase the secret key rate using well known multiplexing techniques by means of microwave photonics technologies [3].

Multiplexed QKD systems have two important goals: increasing the effective key rate and providing simultaneously secret keys to different users. The achievement of these goals is critical in order to spread the use of QKD to current deployed networks, especially in the access and metro areas. Among the reported contributions in the area of multiplexed QKD systems one can find Time Division Multiplexing (TDM)-QKD [4], Wavelength Division Multiplexing (WDM)-QKD [5] and Subcarrier Multiplexing (SCM)-QKD [6]. In principle the WDM-QKD approach is very attractive since it is compatible with the dominant techniques employed in the transmission of classical information channels along current optical networking infrastructures. However, the coexistence of classical and quantum signals, is not straightforward as the Raman effect that classical channels exert over the quantum channels pose a severe limitation. To overcome this limitation initially proposed WDM-QKD systems were configured by placing a single quantum channel in 1310 nm band while allocating the classical channels in 1550 nm band [7]. However, in order to profit from the benefits of Dense WDM technology, alternative approaches have been proposed in which both classical and quantum channels are located in the 1550 band. For instance, the system proposed in [8] reports up to 3 quantum channels with bit rate higher than 200 kb/s while in [9] 4 bidirectional classical-quantum channels coexist in the C band, the classical channels transmitting at 10 Gb/s and quantum channels delivering keys at a rate of ~700 kb/s. In order to achieve these values it is proposed that the classical information and quantum channels travel separately from central node to a distribution point where they are combined and from which they travel together along the last mile to the end user. In this way, the deleterious contribution of the Raman effect is avoided. While this solution is technically feasible there are other QKD multiplexing schemes which require at least one classical reference traveling together with the quantum signal through the same fiber for management and control tasks such as clock recovery, polarization, delay and phase tracking etc. This is the case for instance of Time-bin QKD [5] or SCM-QKD [6] systems.

In this paper we report the design of a hybrid network which can transport classical channels and a high number of quantum channels coexisting with a classical channel which is employed as reference. We experimentally demonstrate the successful transmission of 4 bidirectional classical channels and 40 quantum channels based on SCM-QKD employing standard WDM 100 GHz ITU-Grid. In addition, a separate classical channel is also sent with the quantum channels for monitoring purposes. The transmission rate for the classical channels is 10 Gb/s while the secret key rate for each single quantum channels is 5 kb/s which is limited exclusively by the pulse source rate and the photon counter bandwidth. The quantum channels share fiber with the reference signal, which is launched with enough low power to avoid the Raman effect over the quantum channels.

## 2. Description of the hybrid DWDM quantum and classical transmission

Figure 1 shows the proposed optical network configuration, which was also experimentally implemented. The network allows the combination of the quantum signals with traditional upstream (US) and downstream (DS) channels. Basically, there is a central node (CN) which contains the transmitters (TX) and receivers (RX) of the classical channels for down and

uplink channels, respectively. Also, the quantum channels and reference channel transmitters which are separately sent to a remote node (RN) where they are combined with a classical DWDM multiplexer. Note that all optical sources are located in the CN to permit a reduction of the system complexity [10].

The frequency plan shown in the lower part of the figure illustrates the spectral location of the classical, quantum and reference channels. The system incorporates coarse wavelength multiplexing (CWDM) to combine/separate the different optical bands. The CWDM multiplexer defines three optical bands with a 20 nm separation. The classical reference channel is centered at 1531 nm inside the erbium doped amplifier (EDFA) band as it requires further amplification. Indeed, we perform a double stage of amplification: a first optical stage before photodetection and other electrical stage after photodetection. The optical band centered at 1551 nm is used to transmit the quantum channels and the 1571 nm band is used to provide the US and DS channels. Initially, it could be better to place the classical channels in the 1550 nm band since the losses are lower than 1570 band. However, the FBG filtering stages, which were needed for each quantum channels were fabricated in this band, therefore, the classical channels had to be located in 1570 nm band.

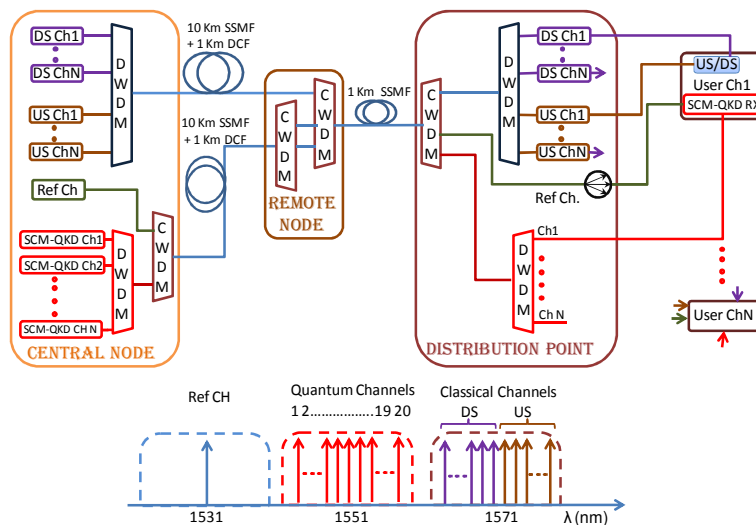


Fig. 1. Optical network schematic with dual feeder fiber architecture and frequency plan.

Classical channels implement a DWDM bidirectional access network providing symmetric downlink and uplink signals. This architecture includes all transmitters in the central node in order to reduce maintenance and costs. Classical channels are multiplexed by means of a DWDM device and sent to the remote node through an optical fiber link. Quantum channels are also DWDM multiplexed, CDWM combined with the reference channel and delivered through a different fiber link to the remote node. The two optical links between CN and RN have identical configurations consisting of a 10 km standard single mode fiber (SMF) followed by a 1 km dispersion compensating fiber (DCF) to avoid the dispersive effects.

The remote node is composed by two Coarse WDM (CWDM) devices one to split the incoming quantum signal from the reference channel and the other to combine the three bands again. Note that the remote node is a last mile solution, featuring a typical length below 2 km. Finally, in the distribution point (DP) there are a set of demultiplexers to split the incoming signals, one DWDM for the US/DS classical channels and another DWDM unit to demultiplex the quantum channels.

### 3. Experimental setup

The experimental setup shown in Fig. 1 combines 4 bidirectional classical channels which transport baseband data at 10 Gb/s and 20 WDM quantum channels based on SCM-QKD technology [6]. Note that each WDM quantum channel contains two SCM quantum channels. We used a commercial CWDM with four optical bands centered at 1531, 1551, 1571 and 1591 nm. Each CWDM band had a bandwidth of 16 nm which allowed the allocation of 20 DWDM channels with 0.8 nm wavelength separation. As mentioned in the previous section the first band was used to transmit the reference channel (1531.12 nm); the next band hosted the 20 WDM quantum channels (1545.3-1557.36 nm) and finally in the third band 4 DS channels (1567.95-1570.42 nm) and 4 US channels (1571.24-1573.71 nm) were inserted.

The transceivers for downlink and uplink were implemented by means of a laser source featuring a 100 MHz bandwidth which was amplitude modulated by using an external modulator biased at quadrature. Additionally, a pseudorandom generator was used to drive the modulator with a 10 Gb/s baseband signal. In the CN, the externally modulated downstream channels and also, the unmodulated optical carriers for the uplink are launched into the network after the DWDM demultiplexer. In this way, a given user will be reached by its own downstream channel and also the corresponding one in the upstream band. They are modulated by the corresponding user's upstream traffic. These channels are modulated by an electro-optic modulator (EOM) and finally launched back to the CN across a circulator simplifying maintenance and costs as corresponds to a remote equipment architecture. Upstream channels are demultiplexed in the CN.

Figure 2 represents a scheme which shows in detail the configuration of the SCM-QKD system [6]. Each quantum channel consists on a transmitter located at the CN and a receiver for each end-user which are named Alice and Bob, respectively. Each quantum transmitter consists on a faint optical source with pulses of a 1.3 ns FWHM and a repetition rate of 1 MHz. The faint pulse laser source located at Alice's side emits at an optical frequency  $\omega_0$  which is externally modulated by using an Amplitude Modulator (AM) which is fed employing independent electrical subcarriers. For parallel key distribution, each subcarrier transmits a different key which is generated by a voltage controlled oscillator (VCO) randomly phase-modulated among four possible values 0,  $\pi$  and  $\pi/2$ ,  $3\pi/2$  which form a pair of conjugate bases required to implement the BB84 protocol. In our experimental setup, two subcarriers are considered coming from VCOs of frequencies  $f_1 = 10$  and  $f_2 = 15$  GHz. To encode the binary secret key in each subcarrier, Alice introduces a random and independent phase shift  $\Phi_{1A}$  and  $\Phi_{2A}$  for each subcarrier. The amplitude modulation generates different optical sidebands corresponding to each electrical subcarrier. Each one corresponds in the time domain to a faint pulse with a given average photon number,  $\mu$ . In this way, the SCM-QKD system is a scheme which encodes the bits by means of the optical sidebands generated in the modulation. As example, Fig. 2(a) shows the probability distribution for a scenario where Alice transmits 2 keys in parallel. In this case, 2 lower and 2 upper sidebands appear around the optical carrier  $\omega_0$  which are named LSB and USB, respectively. The receiver (Bob) has a similar configuration as transmitter (Alice) but in this case the optical signal after propagating through the fiber link is modulated by means of a Phase Modulator (PM). Bob selects the basis for each subcarrier to realize the measurement of the transmitted qubit by synchronously inserting independent random phase shifts  $\Phi_{1B}$  and  $\Phi_{2B}$  (now randomly phase-modulated among values 0 and  $\pi/2$ ). After filtering, the photon detection was realized by placing a Single Photon Avalanche Detector (SPAD) for each optical sideband. The SPADs worked with a detection gate width of 2.5 ns, an efficiency  $\rho$  close to 10% and the dark count probability was  $1.2 \times 10^{-5}$ .

As a consequence of the modulator concatenation, an interference single-photon signal is generated at each one of the sidebands of each subcarrier with a certain probability as shown in Fig. 2(b). For a given subcarrier, if Alice and Bob's bases match, then the photon will be

detected with probability 1 by either the detector placed after the filter centered at USB, or by the detector placed after the filter centered at LSB depending on whether a “0” or a “1” was encoded, respectively. If, on the contrary Bob and Alice’s bases do not match there will be an equal probability of  $\frac{1}{2}$  of detecting the single photon at any of the two detectors and this detection will be discarded in a subsequent procedure of public discussion. Note that Fig. 2(b) plots the measured bits at Bob’s side when the base choices match in all channels corresponding the bits “0” and “1” for the electrical subcarriers  $f_1$  and  $f_2$ , respectively.

A classical reference channel was required to convey a synchronization signal from Alice to Bob and also to stabilize the link against fiber length fluctuations by providing Bob with replicas of the 10 and 15 GHz electrical subcarriers produced at Alice’s side. The reference and quantum channels were combined using a CWDM with 0.5 dB insertion losses to share the same optical fiber link. Upon selection the reference channel is amplified optically (20 dB) and electronically (60 dB) before and after respectively being detected by a PIN diode. From the detected signal the 10 GHz and 15 GHz RF signals, which are employed to modulate the signal received by Bob to implement the BB84 protocol, are regenerated.

We evaluated the photon crosstalk due to the Raman Effect that the reference channel generates in each optical filtering output of Bob’s receiver for the SCM channels of each user, finding out that Raman power signal is reduced below the dark count level if the launched optical power of the reference channel is lower than  $-25$  dBm.

After 1 km fiber transmission, a demultiplexer separated the three bands providing for each user the US/DS channels (not shown in the Fig. 2 for more clarity), the quantum channels and the reference signal.

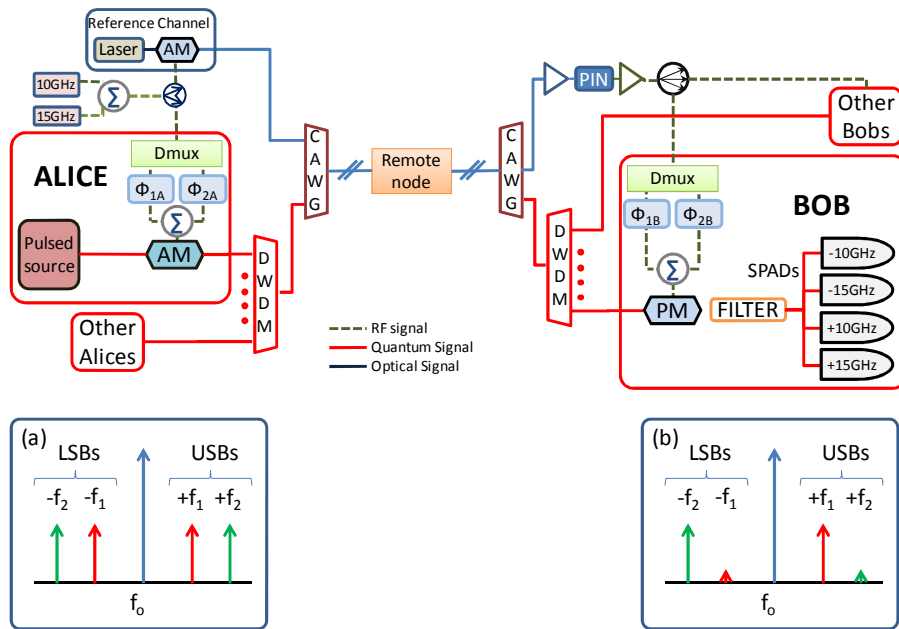


Fig. 2. Scheme of SCM-QKD system for one user integrated on the optical network. Alice (transmitter) is located in the central node and Bob (receiver) acts as end-user. Probability distribution for two bits “0” and “1” corresponding to the electrical subcarriers  $f_1$  and  $f_2$ , respectively, transmitted in parallel at (a) Alice’s side and (b) after detection in Bob’s side measuring in matched basis.

To demonstrate the successful performance of our system, the signal degradation for the classical and quantum channels was measured by employing the bit error rate (BER) as a performance parameter. For the experimental evaluation, DS and US channels were measured in presence of the quantum channels as shown in Fig. 3(a). For comparison, optical back-to-

back (B2B) measurements have been included in Fig. 3 which is similar to all US and DS channels. In Fig. 3(b), we show the corresponding BER measurement when the quantum channels are disabled. As we expected the quantum channels do not affect the classical channels. For both cases, the penalty is around 1.5 dB for the DS due to optical losses and double (3.5 dB) for US due to round trip propagation.

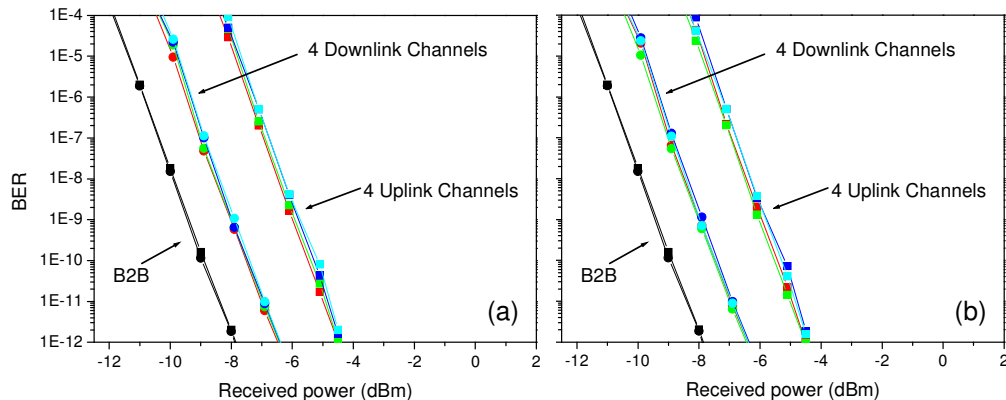


Fig. 3. BER measurement for DS and US channels with quantum channels (a) enabled and (b) disabled. DS channels are located at 1567.95 (●), 1568.11 (●), 1569.59 (●) and 1570.42 nm (●) and US channels are located at 1571.24 (■), 1572.06 (■), 1572.89 (■) and 1573.71 nm (■). Also, B2B is plotted for a DS (●) and US (■) channels.

As shown in Fig. 2, we employed a DWDM to deliver the quantum channels to the final users and, in addition, each user has a filtering stage to select and detect each one of the optical sidebands sent from Alice [11]. This filtering stage based on the cascade of Fiber Bragg Gratings (FBGs) has an extinction ratio (ER) around 20 dB. The extinction ratio composed of the DWDM and the FBG filtering stage determines the total ER and consequently, the quantum BER (QBER) of the system.

In order to evaluate the minimum ER at Bob's side to obtain a suitable QBER, we used a programmable optical processor to provide a DWDM system simulation where the effective ER can be controlled. The procedure consists of the measurement of the QBER for the quantum channel corresponding to the worst case, i.e., the central channel, while adjacent quantum channels are added in function of the ER value imposed by the DWDM setup. In particular, we considered one single channel corresponding to the B2B case and the scenario when 3, 11 and 20 WDM quantum channels are simultaneously transmitted. The ER value of the DWDM channels is modified from 20 to 40 dB being the total ER from 40 to 60 dB.

In Fig. 4(a) and 4(b), we show the QBER as a function of the DWDM ER for each electrical subcarrier corresponding to 10 and 15 GHz, respectively. For high ER values, the contribution of the adjacent channels is small and slight differences are found when 3, 11 or 20 WDM quantum channels are considered. In contrast, low ER values imply that a high number of quantum channels introduce a significant crosstalk increasing the QBER. However, a moderate change in the QBER is found between 3 and 20 quantum channels, which indicates that the first channels are more restrictive in the QBER measurement. Therefore, we can conclude from Fig. 4 that minimum ER to guarantee a QBER close to 2% is around 40 dB for each channel. Note that 40-45 dB can be high for commercial DWDM devices. Consequently, it can be interesting to consider the incorporation of FBGs filters as it occurs in our SCM-QKD systems by combining different FBGs filtering in cascade.

Finally, Fig. 4(c) plots the obtained secret key rates for one single channel (■) and the total value for the previous cases with 3 (●), 11 (▲) and 20 (▼) quantum channels. It is widely known that for BB84 protocol based on weak coherent states, the optimal  $\mu$  against the

most general attack is given by the overall transmittance (including channel transmittance and efficiency of SPADs [2]. This fact implies that the value of  $\mu$  is far from 1. However, the security analysis for SCM-QKD systems based on weak coherent pulses and a *strong reference* against the (most serious) Photon Number Splitting attack, permits a value of  $\mu = 1$  to minimize the fraction of information  $I_E$  that Eve can extract from multiphoton pulses [12]. In this way, the secure key rate  $K_{\text{final}}$  is related to the sifted key rate and the QBER by the following expression [13]:

$$K_{\text{final}} \approx K_{\text{sifted}} \cdot \left\{ \Delta \left[ 1 - h\left(\frac{QBER}{\Delta}\right) \right] - h(QBER) \right\} \quad (1)$$

where  $\Delta = 1 - I_E$  represents the secure fraction in the absence of loss and error and  $h(x)$  is the binary entropy function. We experimentally measure the sifted key rate  $K_{\text{sifted}}$  for each quantum channel and the corresponding experimental value of QBER. Then, we estimate the multiplexed secret key rate by means of the Eq. (1) from the value of each individual WDM quantum channel,  $K_{\text{final}}$ . In Fig. 4(c), we can observe that the secret key rate for a single channel is independent of the DWDM ER since the FBG filtering stage was designed to guarantee a minimum crosstalk for one single channel. However, we can see important differences for ER values lower than 30 dB where the QBER is different for each scenario. For ER values close to 40 dB, we also check that the crosstalk is minimized enough to optimize the transmission of DWDM quantum channels since we increased around 13 dB the secret key rate respect to the single channel.

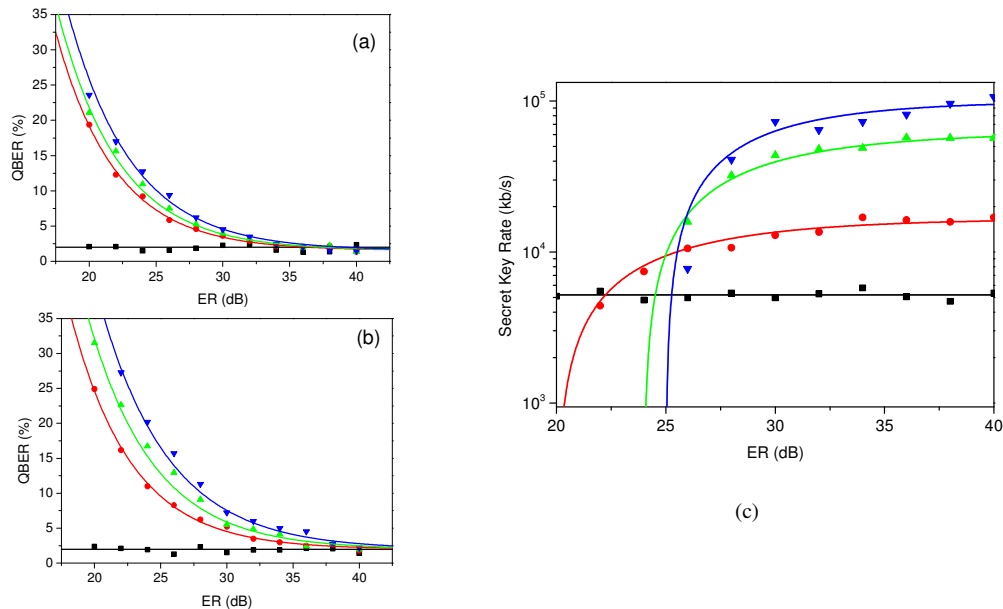


Fig. 4. QBER vs. the extinction ratio for the electrical subcarrier (a) 10 GHz and (b) 15 GHz and the (c) total secret key rate when a single quantum channel (■) and 3 (●), 11(▲) and 20 (▼) WDM quantum channels are enabled.

Note that we experimentally demonstrated moderate single (~5 kbps) and multiplexed (~200 kbps) key rates although the number of DWDM channels is very relevant. The capacity of the systems depends on the QKD terminal equipment used in the optical network which is limited to 1 MHz in our case due to the trigger and deadtime of the SPADs. Using 1 GHz-SPADs [14], the individual and multiplexed secret key rates could be readily increased by 3

orders of magnitude, i.e., 5 Mbps and 200 Mbps, respectively. Obviously, each DWDM quantum channels has available a 50 GHz bandwidth and alternative QKD systems could be used.

#### **4. Conclusion**

We have proposed and implemented, as far as know for first time, an optical network to transport 4x10 Gb/s bidirectional classical channels and 40 quantum channels based on DWDM-SCM-QKD two-tier multiplexing. The transmission key rate was increased in a factor 20 from a SCM quantum channel with a secret key rate close to 5 kb/s. The quantum channels share fiber with the reference signal which travels with enough low power to avoid the Raman effect and they were transmitted with a QBER lower than 2% by controlling the ER of the demultiplexer which suitable value is close to 40 dB for each quantum channel.

#### **Acknowledgments**

The authors wish to acknowledge the financial support of the Spanish Ministry of Science & Innovation and the Generalitat Valenciana through projects CONSOLIDER INGENIO 2010 Quantum Information Technologies and PROMETEO GVA 2008-092 MICROWAVE PHOTONICS.